Thoma et al., http://www.jcb.org/cgi/content/full/jcb.201006059/DC1

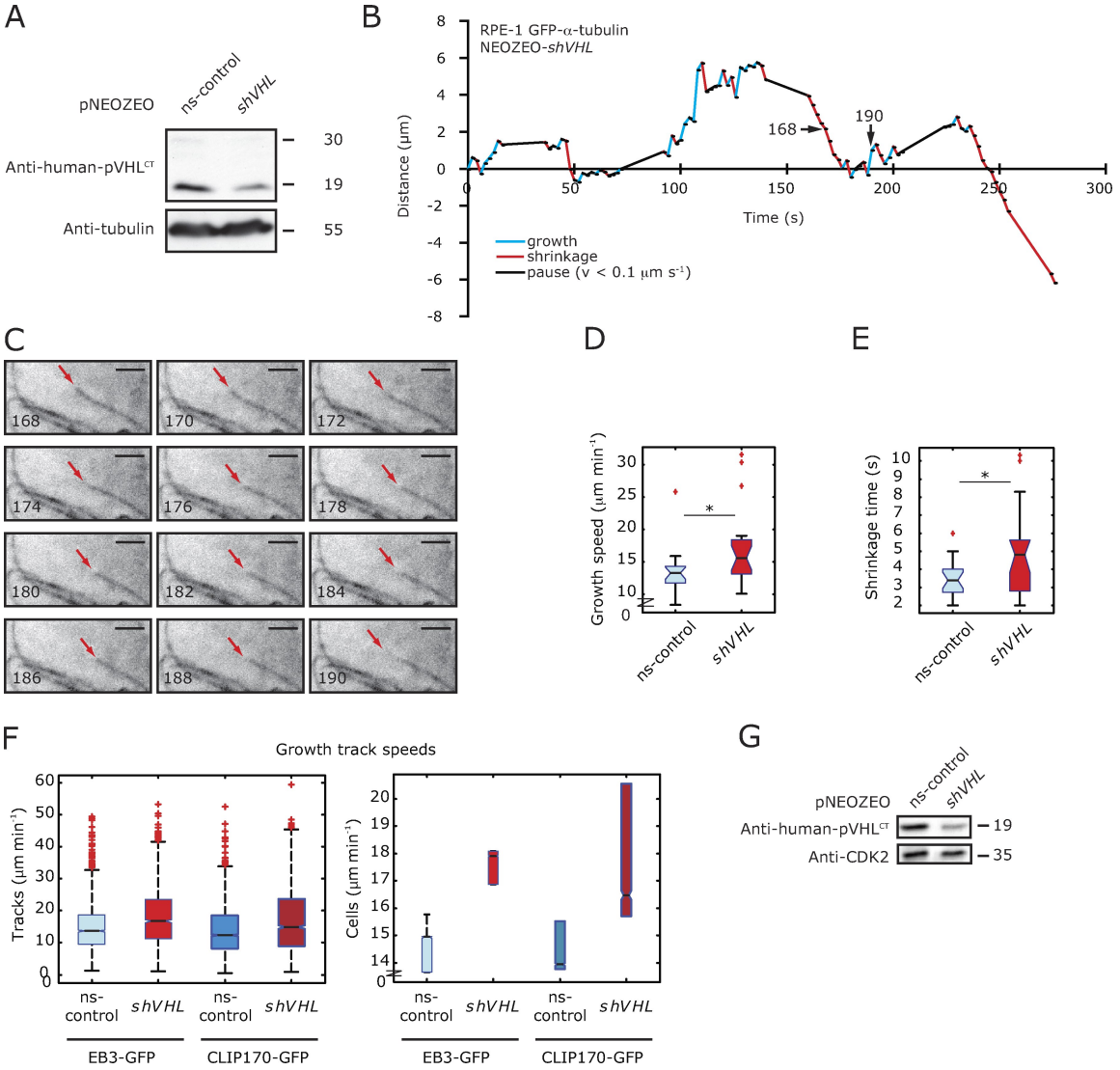

Figure S1. **Manual GFP–α-tubulin tracking in RPE-1 cells depleted for VHL and comparison of automated tracking of EB3-GFP and GFP-CLIP170 as markers of MT growth.** (A) Western blotting of whole-cell lysates of RPE-1 GFP–α-tubulin cells expressing shRNAmir against ns-control and *shVHL* using anti–human pVHL^{CT} antibody. Probing against tubulin served as a loading control. (B) Representative sequence of hand-tracked MT length change in RPE-1 GFP–α-tubulin cells. Growth phases are shown in blue, shrinkage phases are shown in red, and pause phases are shown in black (a pause is defined by a velocity < 0.1 μm s^{-1}). The black arrows indicate the first and last time points of the image series in E. (C) Image series used to track the MT tip (red arrows) between 168 and 190 s. Bars, 2 μm. (D) Distribution of mean growth speed measured by manual tracking of MTs in RPE-1 GFP–α-tubulin cells using box plot representation (*, P < 0.05; permutation *t* test; *n* = 20 MTs each condition). (E) Distribution of mean shrinkage time measured by manual tracking of MTs in RPE-1 GFP–α-tubulin cells using box plot representation (*, P < 0.05; permutation *t* test; *n* = 20 MTs each condition). (F) Box plots showing the growth speed of EB3-GFP and GFP-CLIP170 comets expressed transiently in RPE-1 cells. pVHL was depleted using stable lentiviral transfection (pCMV-NEO-ZEO) of shRNAmir against VHL (*shVHL*) and a nonsilencing control (ns-control). (D–F) Boxes indicate 25, 50 (median), and 75% quantiles; whiskers extend to 1.5× the interquartile range; red dots indicate outliers beyond this range. Notched boxes indicate uncertainty of the median. Boxes whose notches do not overlap indicate that the medians of the two clusters differ at the 5% significance level. (G) Western blotting of whole-cell lysates of RPE-1 cells expressing shRNAmir against ns-control and *shVHL* using anti–human pVHL^{CT} antibody. Probing against CDK2 served as a loading control. (A and G) Molecular mass is indicated in kilodaltons.

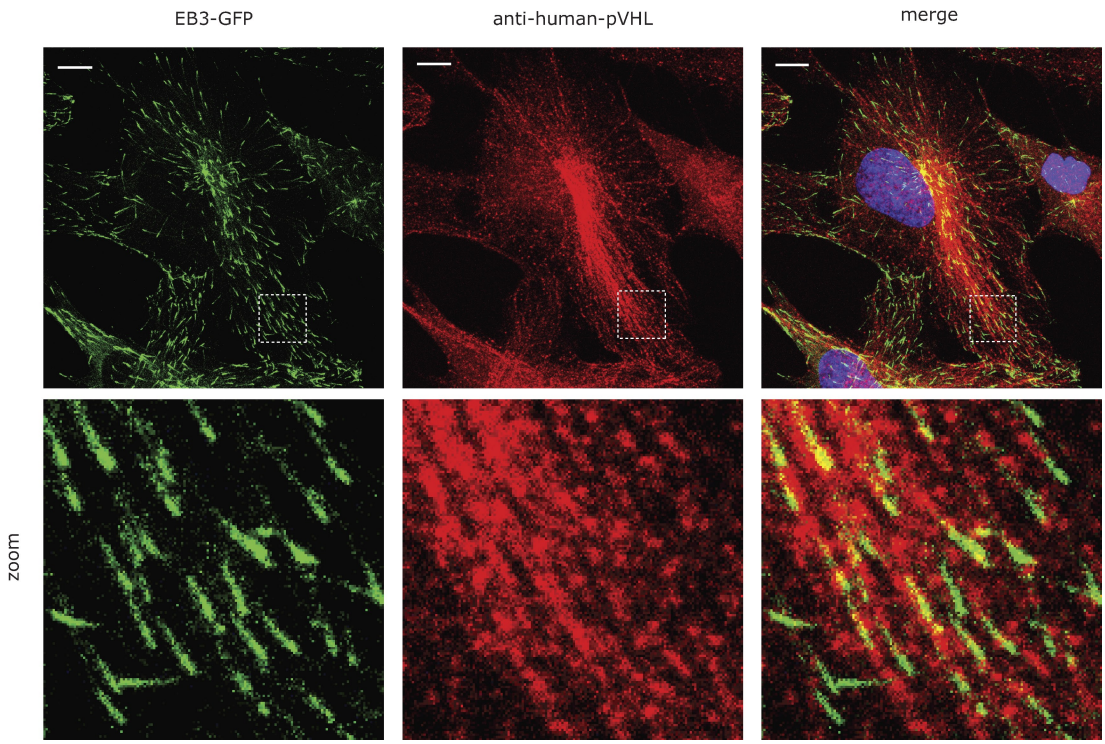

Figure S2. **Colocalization of pVHL and EB3 comets in RPE-1 cells.** Immunofluorescence staining with anti-pVHL^{NT} antibody (red) of RPE-1 cells expressing EB3-GFP. Zoomed images of the boxed areas are shown below. The data show that pVHL decorates the entire MT lattice in a punctate pattern and not specifically at the MT end. Bars, 5 µm.

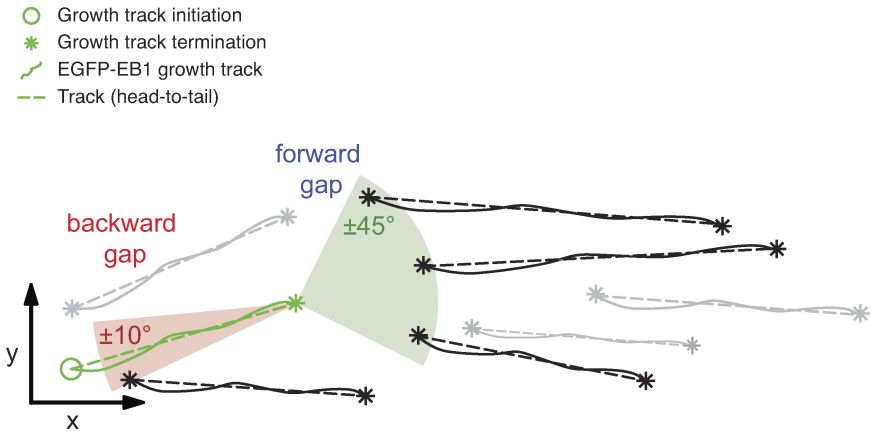

Figure S3. **Grouping of MT growth tracks.** For each termination event of a growth track (green), a forward and backward search cone is constructed to identify potential initiation events of growth tracks in subsequent frames that may belong to the same MT. The search cone for forward gaps is shown in light green with an opening angle of ±45°. The search cone for backward gaps is shown in pink with an opening angle of ±10°. The tracks in black are considered for grouping, whereas growth tracks in light gray have been excluded.

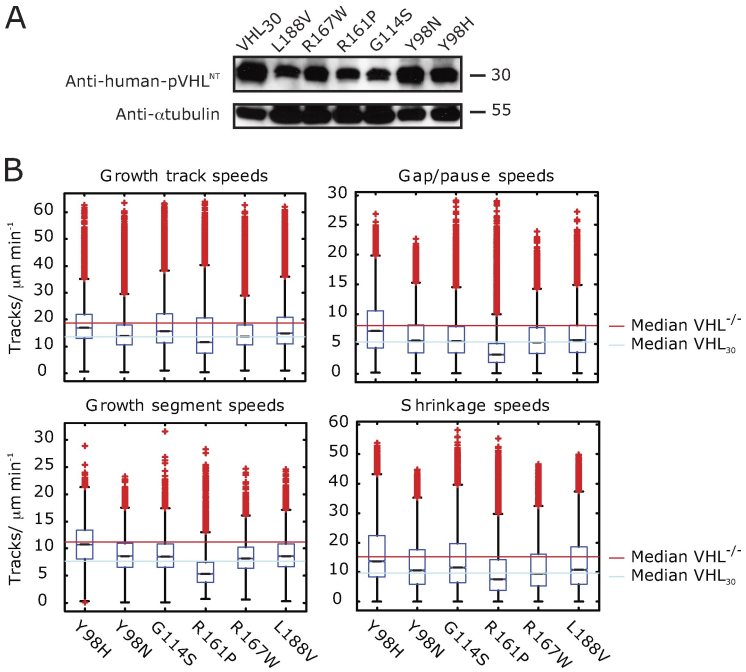

Figure S4. **Analysis of naturally occurring VHL point mutants.** (A) Western blot of whole-cell lysates of RCC-4 cell pools stably transfected with retroviral vectors expressing a set of naturally occurring VHL disease point mutants using anti–human pVHL^{NT} antibody. Probing against tubulin served as a loading control. Molecular mass is indicated in kilodaltons. (B) Box plot representation of the distribution of the measured parameters of MT dynamics (as indicated by the title of panels). The light blue line represents the median value of RCC-4 cells expressing wild-type pVHL$_{30}$, and the red line represents the median value of RCC-4 cells expressing the vector control (VHL$^{-/-}$; Figs. 1 I and 2 D). The MT instantaneous growth speeds, the MT gap/pause speeds, the MT growth segment speeds, and the MT instantaneous shrinkage speeds are measured as explained in Figs. 2 and 3. Boxes indicate 25, 50 (median), and 75% quantiles; whiskers extend to 1.5× the interquartile range; red dots indicate outliers beyond this range. Notched boxes indicate uncertainty of the median. Boxes whose notches do not overlap indicate that the medians of the two clusters differ at the 5% significance level.

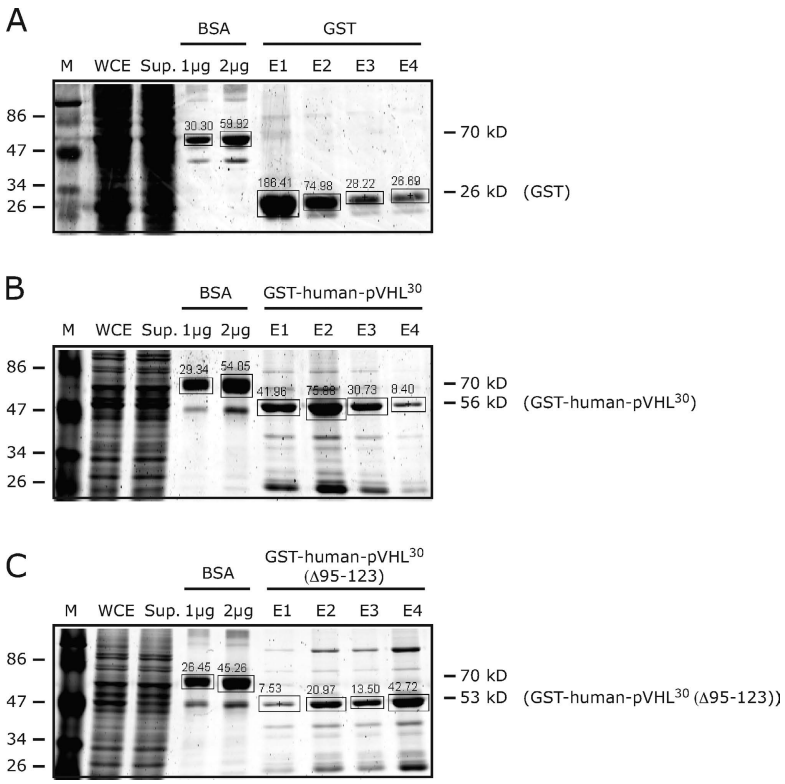

Figure S5. **Purification of GST fusion proteins for GTPase assay.** (A–C) SDS-PAGE and Coomassie staining from purification steps of GST fusion proteins: GST (A), GST–human VHL_{30} (B), and GST–human VHL_{30}(Δ95–123) (C). Protein concentration was measured densitometrically by using the LI-COR Odyssey system and normalized against the BSA standards. Boxes depict the area used for densitometrical assessment of protein quantity. M, protein marker; WCE, Sf9 whole-cell extract; Sup., supernatant after incubation with GST-beads; E1– E4, elutions 1–4 from GST beads.

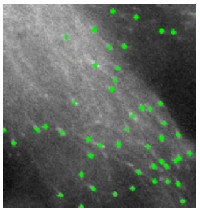

Video 1. **RPE-1 ns-control EB3-GFP comet detection.** This video demonstrates the performance of EB3-GFP comet detection. Raw data are shown in the left panel, and green dots mark the detected EB3-GFP comets in the right panel. The original time-lapse sequence consists of 125 frames acquired with a frame rate of 0.5 s. The replay rate of the videos is 10 frames/s, i.e., a twentyfold acceleration.

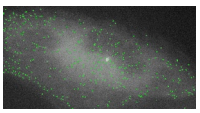

Video 2. **RCC-4 $VHL^{-/-}$ EB3-GFP comet density.** This video indicates the large number and high density of EB3-GFP features captured for a single cell in a typical time-lapse video. Detected events outside the cell region are false positives. They exist for only one to two frames and do not affect the tracking. Green dots indicate the computer-detected positions of EB3 comets. The original time-lapse sequence consists of 125 frames acquired with a frame rate of 0.5 s. The replay rate of the videos is 10 frames/s, i.e., a twentyfold acceleration.

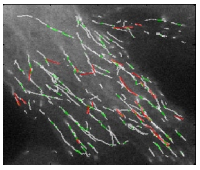

Video 3. **RPE-1 ns-control tracking and grouping.** This video displays the grouped MT growth tracks in the cell region shown in Video 1 as solid lines. Growth tracks are shown in white, forward gaps are shown in green, and backward gaps are shown in red. Note that comets are only tracked within 12 pixels from the border; outside this area, EB3-GFP signals are not detected. The original time-lapse sequence consists of 125 frames acquired with a frame rate of 0.5 s. The replay rate of the videos is 10 frames/s, i.e., a twentyfold acceleration.

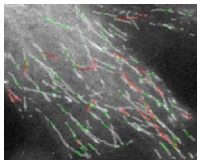

Video 4. **RPE-1 ns-control tracking and grouping.** This video displays a zoom of an area of Video 3. For better comparison and visibility of the underlying EB3-GFP comets, growth tracks are shown in translucent white, forward gaps are shown in translucent green, and backward gaps are shown in translucent red. The original time-lapse sequence consists of 125 frames acquired with a frame rate of 0.5 s. The replay rate of the videos is 10 frames/s, i.e., a twentyfold acceleration.

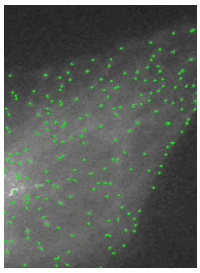

Video 5. **RCC-4 VHL$^{-/-}$/VHL$_{30}$ with 40 nM nocodazole.** This video compares the number of EB3-GFP comets detected after nocodazole perturbation in a cell without (left) and with (right) active VHL. Observe the increased number of growing MTs when VHL is active (right). Green dots indicate the computer-detected positions of EB3 comets. The original time-lapse sequence consists of 125 frames acquired with a frame rate of 0.5 s. The replay rate of the videos is 10 frames/s, i.e., a twentyfold acceleration.

Table S1. **Results of manual GFP–α-tubulin tracking in RPE-1 cells expressing shRNA against VHL (shVHL) or a nonsilencing control hairpin (ns-control)**

Image parameter	RPE-1 expressing GFP–α-tubulin	
	ns-control	shVHL
Number of videos	6	7
Number of MTs	20	20
Growth track speeds (μm min^{-1})	12.5 ± 6.5	15.7 ± 8.5[a]
Shrinkage speeds (μm min^{-1})	13.3 ± 8.5	14.0 ± 12.1
Δ*Tpause* (s)	4.2 ± 3.5	3.2 ± 2.5[a]
Δ*Tgrowth* (s)	3.0 ± 2.6	3.0 ± 1.8
Δ*Tshrink* (s)	3.4 ± 3.1	4.1 ± 5.1[a]

Per condition, number of videos, number of tracked MTs, growth track speeds ± SD, shrinkage speeds ± SD, pause time ± SD, growth time ± SD, and shrinkage time ± SD are shown.

[a]Significant difference between ns-control and shVHL ($P < 0.05$, permutation *t* test).

Table S2. **Results of grouping of visible growth tracks in RPE-1 cells expressing shRNA against VHL (shVHL) and a nonsilencing control hairpin (ns-control)**

Image parameter	RPE-1 expressing EB3-GFP	
	ns-control	shVHL
Number of videos	12	13
Number of growth tracks	68,939	55,286
Grouped tracks (%)	72.7	73.5
Growth track speed (μm min^{-1})	15.4 ± 7.9	17.6 ± 8.1
Gap/pause speed (μm min^{-1})	6.2 ± 3.9	7.2 ± 4.4
Δ*Ttrack* (s)	3.4	3.4
Δ*Tgap* (s)	5.8	5.6
Growth segment speed (μm min^{-1})	8.8 ± 3.3	10.0 ± 3.5
Gaps per growth segment	1.64	1.62
Time ratio *Tgap/Tsegment*	0.48	0.48
Δ*Tsegment* (s)	18.0	17.5
Shrinkage speeds (μm min^{-1})	13.7 ± 10.3	15.4 ± 11.0
Δ*Tshrink* (s)	7.9	8.1
Pshrink (%)	29.4	32.9
Tshrink (%)	25.2	30.3

Per condition, number of videos, number of visible growth tracks, percentage of grouped tracks, growth track speeds ± SD, gap/pause speeds ± SD, growth track time, gap/pause time growth segment speeds ± SD, number of gaps/pauses per growth segment, percentage of time spent in gap/pause within a growth segment, growth segment time, shrinkage speeds ± SD, shrinkage time, probability of shrinkage at the end of grouped growth track, and percentage of time spent in shrinkage within a multitrack trajectory are shown.

Table S3. **Results of grouping of visible growth tracks in RCC-4 cells naturally lacking pVHL expression reconstituted with retroviral expression (pCMV(R)) of the wild-type long form $pVHL_{30}$, the wild-type short form $pVHL_{19}$, and the empty vector as control ($VHL^{-/-}$)**

Image parameter	RCC-4: expressing EB3-GFP and retroviral expression of		
	empty control	VHL_{30}	VHL_{19}
VHL state	$VHL^{-/-}$	Wild-type long form	Wild-type short form
Number of videos	10	9	12
Number of tracks	37,120	41,844	28,578
Grouped tracks (%)	73.5	73.3	63.7
Growth track speed (μm min^{-1})	18.7 ± 7.1	14.8 ± 7.4	16.8 ± 7.8
Gap/pause speed (μm min^{-1})	8.3 ± 4.7	6.0 ± 3.6	6.3 ± 4.0
Δ*Ttrack* (s)	3.5	3.3	3.0
Δ*Tgap* (s)	5.0	5.5	6.0
Growth segment speed (μm min^{-1})	11.6 ± 3.8	8.5 ± 3.2	9.0 ± 3.4
Gaps per growth segment	1.60	1.74	1.52
Time ratio *Tgap/Tsegment*	0.45	0.48	0.50
Δ*Tsegment* (s)	16.5	17.8	16.1
Shrinkage speed (μm min^{-1})	16.9 ± 10.7	12.6 ± 9.5	14.2 ± 10.6
Δ*Tshrink* (s)	8.4	7.8	8.1
Pshrink (%)	29.3	21.9	24.6
Tshrink (%)	28.6	18.6	22.1

Per condition, number of videos, number of visible growth tracks, percentage of grouped tracks, growth track speeds ± SD, gap/pause speeds ± SD, growth track time, gap/pause time growth segment speeds ± SD, number of gaps/pauses per growth segment, percentage of time spent in gap/pause within a growth segment, growth segment time, shrinkage speeds ± SD, shrinkage time, probability of shrinkage at the end of grouped growth track, and percentage of time spent in shrinkage within a multitrack trajectory are shown.

Table S4. **Results of grouping of visible growth tracks of RCC-4 cells reconstituted with the empty retroviral expression vector pCMV(R) ($VHL^{-/-}$) or with pCMV(R) expressing wild-type pVHL (VHL_{30}) treated with nocodazole for the indicated time**

Image parameter	RCC-4: expressing EB3-GFP and retroviral expression of							
	Empty control	Empty control	Empty control	Empty control	VHL_{30}	VHL_{30}	VHL_{30}	VHL_{30}
VHL state	$VHL^{-/-}$	$VHL^{-/-}$	$VHL^{-/-}$	$VHL^{-/-}$	wild-type long form	wild-type long form	wild-type long form	wild-type long form
Time after nocodazole addition (s)	0	20	120	360	0	20	120	360
Number of videos	11	10	9	5	12	12	12	10
Number of tracks	29,993	11,206	4,519	1,029	20,091	19,883	11,458	4,325
Grouped tracks (%)	69.6	53.6	40.1	24.2	62.0	62.0	46.2	28.9
Growth track speed (μm min^{-1})	16.4 ± 8.4	12.7 ± 6.2	10.6 ± 5.2	9.6 ± 5.4	13.4 ± 5.8	14.1 ± 7.3	11.6 ± 6.3	11.0 ± 7.0
Gap/pause speed (μm min^{-1})	6.4 ± 3.7	5.2 ± 2.9	4.3 ± 2.4	3.3 ± 1.6	6.5 ± 3.4	5.6 ± 3.1	4.3 ± 2.6	3.0 ± 2
Δ*Ttrack* (s)	3.1	2.9	2.8	2.6	3.4	3.0	2.8	2.5
Δ*Tgap* (s)	5.4	5.2	5.2	6.2	4.3	5.2	5.6	7.0
Growth segment speed (μm min^{-1})	9.1 ± 3.1	7.3 ± 2.6	6.0 ± 2.2	4.7 ± 1.6	8.9 ± 2.8	7.8 ± 2.8	6.2 ± 2.5	4.6 ± 2.1
Gaps per segment	1.57	1.44	1.28	1.11	1.46	1.52	1.36	1.19
Time ratio *Tgap/Tsegment*	0.47	0.46	0.45	0.49	0.39	0.47	0.49	0.54
Δ*Tsegment* (s)	15.8	14.2	12.8	12.7	14.2	15.0	14.4	13.8
Shrinkage speed (μm min^{-1})	14.9 ± 11.0	10.6 ± 8.4	8.1 ± 7.1	4.7 ± 3.4	11.9 ± 8.4	12.3 ± 10.0	9.1 ± 7.5	7.9 ± 7.6
Δ*Tshrink* (s)	7.3	7.5	7.3	7.4	8.4	7.4	7.4	6.3
P*shrink* (%)	23.7	15.4	12.6	18.9	17.2	18.0	13.4	24.9
T*shrink* (%)	19.4	12.4	10.2	21.1	15.8	14.7	10.5	16.7

Per condition, number of videos, number of visible growth tracks, percentage of grouped tracks, growth track speeds ± SD, gap/pause speeds ± SD, growth track time, gap/pause time growth segment speeds ± SD, number of gaps/pauses per growth segment, percentage of time spent in gap/pause within a growth segment, growth segment time, shrinkage speeds ± SD, shrinkage time, probability of shrinkage at the end of grouped growth track, and percentage of time spent in shrinkage within a multitrack trajectory are shown.

Table S5. **Results of grouping of visible growth tracks of naturally occurring pVHL point mutants in RCC-4 cells**

Image parameter	RCC-4: expressing EB3-GFP and retroviral expression of					
	Y98H	Y98N	G114S	R161P	R167W	L188V
Disease class	2A	2B	2B	2B	2B	2C
Number of videos	10	12	15	14	15	14
Number of tracks	41,865	53,626	40,352	42,838	48,929	35,497
Grouped tracks (%)	72.6	72.4	64.3	47.7	64.1	64.8
Growth track speed (μm min^{-1})	18.2 ± 7.7	15.1 ± 6.9	17.7 ± 8.9	15.0 ± 10.1	15.1 ± 6.9	16.9 ± 8.3
Gap/pause speed (μm min^{-1})	7.8 ± 4.5	6.1 ± 3.6	6.1 ± 3.7	4.3 ± 3.9	5.8 ± 3.3	6.2 ± 3.6
Δ*Ttrack* (s)	3.3	3.4	2.8	2.4	3.2	2.8
Δ*Tgap* (s)	5.2	5.5	6.1	7.7	5.6	5.7
Growth segment speed (μm min^{-1})	10.8 ± 3.8	8.9 ± 3.2	8.9 ± 3.3	6.1 ± 3.4	8.4 ± 2.9	8.9 ± 3.2
Gaps per segment	1.59	1.68	1.57	1.33	1.56	1.57
Time ratio *Tgap/Tsegment*	0.47	0.47	0.52	0.58	0.47	0.51
Δ*Tsegment* (s)	16.5	17.7	16.3	15.6	16.2	15.8
Shrinkage speed (μm min^{-1})	16.3 ± 10.8	13.0 ± 9.4	14.7 ± 11.1	10.9 ± 10.1	12.1 ± 9.2	13.7 ± 10.5
Δ*Tshrink* (s)	8.2	8.0	7.7	7.2	8.0	7.8
P*shrink* (%)	28.8	21.7	27.0	35.4	20.2	26.9
T*shrink* (%)	27.2	18.4	24.0	28.9	17.4	24.0

Per condition, disease class of the mutant, number of videos, number of visible growth tracks, percentage of grouped tracks, growth track speeds ± SD, gap/pause speeds ± SD, growth track time, gap/pause time growth segment speeds ± SD, number of gaps/pauses per growth segment, percentage of time spent in gap/pause within a growth segment, growth segment time, shrinkage speeds ± SD, shrinkage time, probability of shrinkage at the end of grouped growth track, and percentage of time spent in shrinkage within a multitrack trajectory are shown.